applied sciences

MDPI

Article

Investigating the In Vitro Osteogenic Properties of the Inclusion Nanocarrier of Icariin with Beta-Cyclodextrin-Alginate

Somang Choi [1,2,†], Yeong Seok Lee [3,4,†], Han-Saem Jo [5], Woong Kyo Jeong [6], Hak-Jun Kim [1], Mi Hyun Song [1,*], Kyeongsoon Park [5,*] and Sung Eun Kim [1,*]

1 Department of Orthopedic Surgery and Rare Diseases Institute, Korea University Guro Hospital, #148, Gurodong-ro, Guro-gu, Seoul 08308, Korea; chlthakd1029@naver.com (S.C.); dakjul@korea.ac.kr (H.-J.K.)
2 Department of Biomedical Science, College of Medicine, Korea University, Anam-dong, Seongbuk-gu, Seoul 02841, Korea
3 Department of Orthopedic Surgery, College of Medicine, Korea University, Anam-dong, Seongbuk-gu, Seoul 02841, Korea; prince042@hanmail.net
4 Saint Luke Hospital, #726, Tongil-ro, Eunpyeong-gu, Seoul 03368, Korea
5 Department of Systems Biotechnology, Chung-Ang University, Anseong-si, Gyeonggi-do 17546, Korea; luchiatkfkd@naver.com
6 Department of Orthopedic Surgery, Korea University Anam Hospital, #73, Goryeodae-ro, Seongbuk-gu, Seoul 02841, Korea; drshoulder@korea.ac.kr
* Correspondence: wwiiw@hanmail.net (M.H.S.); kspark1223@cau.ac.kr (K.P.); sekim10@korea.ac.kr (S.E.K.); Tel.: +82-2-2626-3239 (M.H.S.); +82-31-670-3357 (K.P.); +82-2-2626-1999 (S.E.K.)
† These authors contributed equally to this work.

Received: 28 May 2020; Accepted: 15 June 2020; Published: 16 June 2020

Abstract: In this study, we created an inclusion nanocarrier of icariin (ICA) and β-cyclodextrin-alginate conjugate (ICA/β-CD-ALG) and determined its in vitro osteogenic ability on MC3T3-E1 cells. The morphological shape of the prepared β-CD-ALG with or without ICA was nano-sized and round. The use of β-CD-ALG achieved a sustained ICA release for up to 7 days. In vitro studies found that ICA/β-CD-ALG had a greater potential in osteogenesis on MC3T3-E1 cells compared to β-CD-ALG by exhibiting both higher alkaline phosphatase levels and the amount of calcium deposits. Moreover, ICA/β-CD-ALG greatly increased the levels of osteogenesis markers including osteocalcin (OCN) and osteopontin (OPN). Our results suggest that ICA/β-CD-ALG plays a significant role in cellular osteogenic activity.

Keywords: icariin; β-cyclodextrin-alginate; drug delivery; MC3T3; osteogenic activity

1. Introduction

Bone defects, which can occur in the setting of trauma and fracture, can lead to local disorders and serious problems for public health [1,2]. Autografts are the unsurpassable method in the treatment of bone defects owing to their osteoconductive, osteoinductive, and osteogenic properties. Allografts with osteoconductive and osteoinductive properties have been used in other bone grafts. However, such allografts have restrictions due to the limited supply, the morbidity at the graft donor sites, blood loss, and disease transmission [3–5].

Cyclodextrins (CDs) are classified as macrocyclic oligosaccharides composed of α-(1→4) linked D-glucopyranose units [6]. Three common CDs such as α, β, and γ-CDs are composed of 6, 7, and 8 glucose units, respectively. CDs are potential candidates in the treatment of bone defects because they can be used as functional carrier materials in complex pharmaceutical formulations [7,8]. CDs have

been broadly applied in pharmaceutical manufacturing since the first pharmaceutical formulation of prostaglandin E2/β-CD manufactured in Japan in 1976 [9]. CDs are able to incorporate suitable guest molecules (small molecules, ions, proteins, and oligonucleotides), inside their hydrophobic cavity resulting in better stability, higher water solubility, and increased bioavailability [10–14]. Recently, a new drug delivery system has emerged that combines different carriers with herbal molecules. This system improves the bioavailability and therapeutic potency of bioactive substances, which are physiological targets, without losing integrity or bioactivity [15].

Epimedii Herba (YinYangHou in Chinese) has been used to treat heart disease, osteoporosis, and rheumatism [16,17]. Icariin (ICA) extracted from *Epimedii Herba* is a major active flavonoid glycoside and has anti-oxidant, anti-inflammatory, and lipid-modulatory efficacies [16,17]. In particular, it has been extensively shown to promote bone healing, such as in postmenopausal osteoporosis. Previous studies reported that ICA not only stimulated the proliferation of rat bone marrow-derived mesenchymal stem cells (MSCs) through ERK and MAPK signaling, but also promoted osteogenic differentiation of rat MSCs via vitalizing the PI3K-AKT-cGMP-PKG pathway [18,19]. Ye et al. recently revealed that ICA induced the proliferation and osteogenic differentiation of rat adipose-derived stem cells via the activation of RhoA-TAZ pathway [16]. Furthermore, Liu et al. showed that ICA-immobilized poly(L-lactide) fibrous membranes enhanced osteogenic activity on MC3T3-E1 cells [17]. Recently, accumulating evidence has showed that ICA plays critical roles in bone regeneration. However, its short half-life, toxic adverse effects, and poor biocompatibility are of concern with regard to its clinical relevance for bone repair [20].

Alginate (ALG) has been developed as a platform for drug delivery systems due to its good cytocompatibility, biodegradation, and biocompatibility [21]. In addition, owing to its chemical versatility, it can be further modified with various molecules via chemical conjugation [22]. In the current study, we developed a controlled delivery system for ICA using a β-CD-conjugated alginate (β-CD-ALG) nanocarrier to overcome the limitations of ICA. Moreover, we investigated the in vitro osteogenic potency of ICA/β-CD-ALG nanocarrier by analyzing alkaline phosphatase (ALP) levels, the amount of calcium deposits, and the levels of osteogenesis markers of MC3T3-E1 cells.

2. Materials and Methods

2.1. Fabrication of β-CD-Alginate (β-CD-ALG) Nanocarrier

The β-CD-ALG nanocarrier was synthesized according to the described methods by Kim et al. [23]. To modify aminated-ALG, 459 mg of ALG (Junsei Chemical Co. Ltd., Tokyo, Japan) and 331.5 mg of 4-(4,6-dimethoxy-1,3,5-triazin-2-yl)-4-methylmorpholinium chloride (DMT-MM, Sigma-Aldrich, St. Louis, MO, USA) were dissolved in 100 mL distilled water (DW). Ethylenediamine (8.19 mg, Sigma-Aldrich, St. Louis, MO, USA) was then added to the ALG solution and reacted for two days. The aminated-ALG was dialyzed using a dialysis membrane (MWCO 12–14 kDa, Spectrum®, CA, USA) against excess DW and lyophilized.

To synthesize the carboxylated β-CD, 15 g of β-CD was dissolved in 100 mL of anhydrous dimethylformamide (Sigma-Aldrich), followed by addition of succinic anhydride (1323 mg, Sigma-Aldrich, St. Louis, MO, USA). The mixtures were reacted under nitrogen conditions for two days. The product was washed three times with DW, centrifuged at 3000 rpm for 10 min at 4 °C, and then dried at 40 °C for three days.

To fabricate β-CD-ALG conjugates, the carboxylated β-CD (300 mg) and DMT-MM (220.8 mg) were dissolved in DW (30 mL) for 1 h. Aminated-ALG (150 mg) was then slowly added to the carboxylated β-CD solution. The reaction was conducted for three days and the resulting solution was dialyzed against DW (MWCO 12,000–14,000) and lyophilized.

2.2. Preparation of ICA-Loaded β-CD-ALG (ICA/β-CD-ALG)

To prepare ICA/β-CD-ALG, different concentrations of 1, 5, or 10 μM of ICA (Purity: >96%, Tokyo Chemical Industry (TCI), Tokyo, Japan) in dimethyl sulfoxide (DMSO, Sigma-Aldrich) were carefully added dropwise to the β-CD-ALG (10 mg/mL) dissolved in DW and stirred for 24 h. The resultant solution was transferred into a dialysis bag (MWCO 3500), dialyzed against DW for three days, and lyophilized. ICA (1, 5, or 10 μM)-loaded β-CD-ALG are henceforth referred to as ICA (1 μM)/β-CD-ALG, ICA (5 μM)/β-CD-ALG, and ICA (10 μM)/β-CD-ALG.

2.3. Characterizations

^{1}H-NMR spectroscopy was performed to confirm the synthesis of β-CD-ALG. The NMR spectrum of β-CD-ALG was recorded in D_2O at 25 °C using a 400 MHz AVANCE IIII HD 400 NMR spectrometer (Bruker Ltd., Manning Park Billerica, MA, USA). The morphologies of β-CD-ALG, ICA (1 μM)/β-CD-ALG, ICA (5 μM)/β-CD-ALG, and ICA (10 μM)/β-CD-ALG were examined using a transmission electron microscope (TEM, JEM-F200, JEOL Ltd., Tokyo, Japan). Prior to TEM analysis, each sample (10 μg) was added to 1 mL of EtOH and sonicated using a Powersonic 405 (bath-type instruments; 40 KHz, power: 350 W, Hwashin Tech Co., Ltd., Seoul, Korea) for 1 h at 4 °C. Then, each sample was transferred to a copper TEM grid (CF200-Cu, Electron Microscopy Sciences, Hatfield, PA, USA) and the morphologies of each sample were acquired with TEM at 200 kV of acceleration voltage.

To conduct particle size analysis using dynamic light scattering (DLS), each sample (100 μg) was added into DW (1 mL) and sonicated for 1 h at 4 °C. The particle sizes and zeta potential values were obtained using a particle size analyzer (Malvern Panalytical Ltd, Malvern, UK) equipped with a He-Ne laser (633 nm). Also, each sample was analyzed with a Nicolet Avatar 360 Fourier transform infrared (FT-IR) instrument (Thermo Electron Corp., Madison, WI, USA).

2.4. In Vitro ICA Release

To examine in vitro ICA release from ICA (1 μM)/β-CD-ALG, ICA (5 μM)/β-CD-ALG, and ICA (10 μM)/β-CD-ALG, each sample (10 mg) dispersed in 1 mL of PBS solution (pH 7.4) was added into a dialysis membrane (MWCO 6~8 kDa). Each bag with the sample was carefully placed into a 15 mL tube containing 5 mL of PBS and then shaken at 100 rpm at 37 °C. At predetermined time intervals, the PBS solution was collected and changed with the same volume of fresh PBS. The released amount of ICA was analyzed using a Flash Multimode Reader (Varioskan™, Thermo Scientific Inc., Waltham, MA, USA) at 290 nm.

2.5. Cytotoxicity

To decide the cytotoxicity of β-CD-ALG, ICA (1 μM)/β-CD-ALG, ICA (5 μM)/β-CD-ALG, and ICA (10 μM)/β-CD-ALG, each group was scattered into a cell culture medium (DMEM) containing 10% FBS and 1% antibiotics (100 U/mL penicillin and 0.1 mg/mL streptomycin). The MC3T3-E1 cells (1×10^4 cells/well, Korean Cell Line Bank, Seoul, Korea) were seeded and incubated into a 96-well plate. After treating with each sample for 24 h, the cells were washed three times with fresh culture medium and further incubated with 10 μL of 1-(4,5-dimethylthiazol-2-yl)-3,5-diphenyl formazan reagent (Sigma-Aldrich) for 4 h in dark conditions at 37 °C. Then, 150 μL of dimethyl sulfoxide (DMSO, Sigma-Aldrich) was added into each well to dissolve the formed formazan crystals. The optical density at 595 nm was detected using a Flash Multimode Reader.

2.6. Cell uptake of β-CD-ALG

Prior to visualize internalization of β-CD-ALG into cells, fluorescein-labeled β-CD-ALG (FITC/β-CD-ALG) was prepared as follows. β-CD-ALG (10 mg) and FITC (2 mg) were added to DW (100 mL) and stirred for one day. Then, the resulting product was obtained by dialysis against

DW and freeze-drying. To investigate cellular uptake of FITC/β-CD-ALG, the cells (1×10^4 cells/well) were added and further cultured into a glass bottom dish (12 mm diameter) overnight. Next, the cells were exposed to FITC/β-CD-ALG (100 μg/mL) for 8 h and then fixed with 4% glutaraldehyde for 30 min. To stain F-actin and the cell nuclei, rhodamine-phalloidin (Thermo Fisher Scientific Inc., MO, USA) and 4-6-diamidino-2-phenylindole (DAPI, Thermo Fisher Scientific, USA) were further added to the cells to stain F-actin and the cell nuclei for 30 min. The cells were observed under a confocal laser scanning microscope (LSM700, Zeiss, Germany).

2.7. ALP Activity

After the cells (1×10^5 cells/well/mL) were cultured in 24-well plates, each sample (100 μg/mL) was treated. At 3 day and 9 day time points, lysis buffer (1× RIPA buffer) was added to each well to perform cell lysis. After centrifugation of the collected cell lysates at 13,500 rpm for 10 min, the supernatant was mixed with *p*-nitrophenyl phosphate (Sigma-Aldrich, USA) solution and reacted at 37 °C for 30 min. Then, the reaction was stopped by adding 1 N NaOH (500 μL) solution. The optical density was measured at 405 nm using a Flash Multimode Reader.

2.8. Calcium Deposition

In the calcium content experiment, we used the same concentrations of cells and β-CD-ALG (with or without ICA) as in the ALP experiment. At 7 day and 21 day time points, the cells were treated with 500 μL of 0.5 N HCl at 37 °C. After overnight incubation, a calcium standard solution (20 μL) was mixed with each sample solution (20 μL) with further addition of 400 μL of blending solution including *o*-cresolphthalein complexone (Sigma-Aldrich) and 8-hydroxy-quindine (Sigma-Aldrich) for 1 min. After additionally treating with 20 μL of 2-amino-2-methyl-1-propanol (AMP) buffer, these mixtures were then reacted for 15 min at RT. The resultant solution (200 μL) was carefully transferred into 96-well plates. The optical density was monitored at 575 nm.

2.9. Osteogenic Gene Markers

The osteogenic ability of β-CD-ALG with or without ICA was also examined by measuring the levels of osteogenic genes including osteocalcin (OCN) and osteopontin (OPN) in cells using real-time PCR. After seeding the cells at a density of 1×10^5 cells/well/mL into a 24-well culture plates, the cells were treated with β-CD-ALG nanocomplexes with or without ICA (100 μg/mL). At 7 day and 21 day time points, total RNA was isolated from the collected cells using the RNeasy Plus mini kit. After determining the RNA levels, 1 μg of total RNA was reverse-transcribed into cDNA. The target genes' primer sequences are described in the Supplementary Materials (Table S1). The PCR amplification and detection tests were conducted as described in Supplementary Materials.

2.10. Statistical Analysis

All data are expressed as mean ± standard deviation. Statistical analysis was carried out via one-way analysis of variance (ANOVA) using Systat software (Chicago, IL, USA). Differences were considered to be significant when p values were less than 0.01 and 0.05.

3. Results

3.1. Physicochemical Characterization of β-CD-ALG with or without ICA

β-CD-ALG was synthesized by reacting aminated ALG with carboxylated β-CD, and synthesis of β-CD-ALG was analyzed with proton NMR. In Figure 1 for the proton NMR spectrum of β-CD-ALG, proton peaks at 4.93 ppm were assigned to –CH of β-CD and ALG. Multiple peaks that ranged from 3.15 to 4.12 ppm signified protons of β-CD and ALG. In addition, methylene proton peaks from aminated ALG were detected at 2.76 ppm.

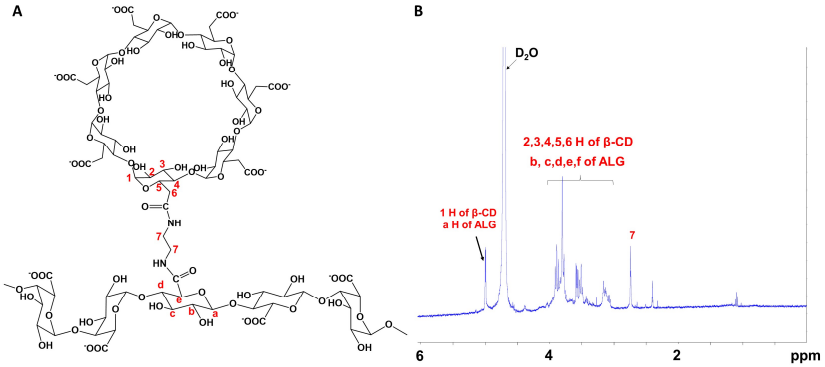

Figure 1. (**a**) β-cyclodextrin-alginate (β-CD-ALG) structure. (**b**) The proton nuclear magnetic resonance (^{1}H-NMR) spectrum of β-CD-ALG.

Hydrodynamic particle sizes and polydispersity indices (PDI) of β-CD-ALG with or without ICA (monitored by dynamic light scattering) were as follows: 436.80 ± 75.95 nm and −30.47 ± 0.8 mV for β-CD-ALG, 439.30 ± 77.45 nm and −16.77 ± 3.6 mV for ICA (1 μM)/β-CD-ALG, 485.00 ± 128.50 nm and −15.37 ± 3.8 mV for ICA (5 μM)/β-CD-ALG, and 467.10 ± 67.00 nm and −9.23 ± 2.0 mV for ICA (10 μM)/β-CD-ALG, respectively. Figure 2 exhibits the β-CD-conjugated alginate (β-CD-ALG) and ICA/β-CD-ALG measured using ATR-FTIR spectra. The FT-IR spectra of β-CD-ALG, β-CD demonstrated major special peaks at 3300–3400 cm^{-1}, 2,854 cm^{-1}, 1,153 cm^{-1}, and 1,029 cm^{-1}. These peaks correspond to the stretching of O–H, CH_2, and C–C and the bending vibration of O–H, respectively. After inclusion of ICA on β-CD-ALG, the ATR-FTIR spectra showed characteristic absorptions for carbonyl (1652 cm^{-1}) and aromatic (1598 cm^{-1}, 1509 cm^{-1}, and 1073 cm^{-1}) moieties in ICA. The estimated ICA loading amount (efficiency) was 22.14 ± 3.37 μg (36.89 ± 5.62%) for ICA (1 μM)/β-CD-ALG, 85.67 ± 3.29 μg (28.56 ± 1.10%) for ICA (5 μM)/β-CD-ALG, and 195.09 ± 5.39 μg (32.52 ± 0.90%) for ICA (10 μM)/β-CD-ALG.

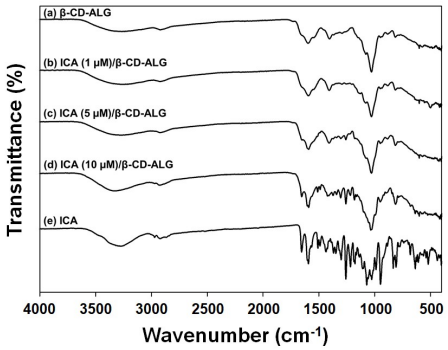

Figure 2. FT-IR spectra of (**a**) β-CD-ALG, (**b**) ICA (1 μM)/β-CD-ALG, (**c**) ICA (5 μM)/β-CD-ALG, (**d**) ICA (10 μM)/β-CD-ALG, and (**e**) ICA.

The morphologies of β-CD-ALG with or without ICA are depicted by the TEM images in Figure 3. All samples were nano-sized by spherical type.

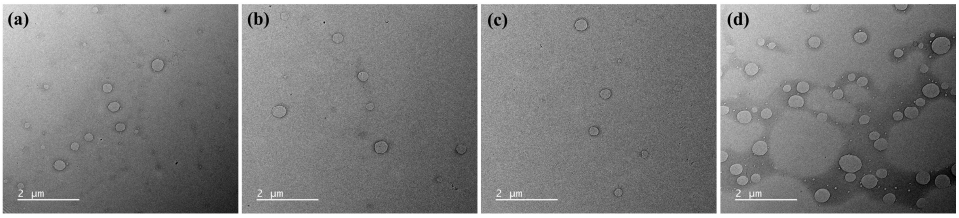

Figure 3. TEM images of (**a**) β-CD-ALG, (**b**) ICA (1 μM)/β-CD-ALG, (**c**) ICA (5 μM)/β-CD-ALG, and (**d**) ICA (10 μM)/β-CD-ALG. Scale bar: 2 μm.

3.2. In Vitro ICA Release

Figure 4 shows the in vitro cumulative ICA release from ICA (1 μM)/β-CD-ALG, ICA (5 μM)/β-CD-ALG, and ICA (10 μM)/β-CD-ALG for 7 days. After one day, the total amounts and percentages of ICA released from ICA (1 μM)/β-CD-ALG, ICA (5 μM)/β-CD-ALG, and ICA (10 μM)/β-CD-ALG were 10.82 ± 1.35 μg (48.86 ± 6.11%), 49.02 ± 3.43 μg (57.22 ± 4.00%), and 119.33 ± 5.54 μg (61.17 ± 2.84%), respectively. Over the 7-day period, 15.83 ± 1.89 μg (71.51 ± 8.53%), 69.01 ± 1.16 μg (80.55 ± 1.36%), and 157.31 ± 7.60 μg (80.63 ± 3.89%) of ICA were released from ICA (1 μM)/β-CD-ALG, ICA (5 μM)/β-CD-ALG, and ICA (10 μM)/β-CD-ALG, respectively.

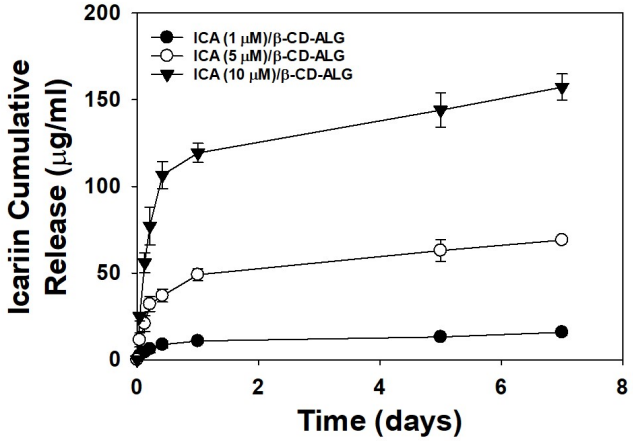

Figure 4. In vitro cumulative icariin (ICA) release from ICA (1 μM)/β-CD-ALG, ICA (5 μM)/β-CD-ALG, and ICA (10 μM)/β-CD-ALG (n = 4 per group).

3.3. Cytotoxic Test and Intracellular Uptake

As shown in Figure 5a, cytotoxicity tests of β-CD-ALG, ICA (1 μM)/β-CD-ALG, ICA (5 μM)/β-CD-ALG, and ICA (10 μM)/β-CD-ALG were performed using MC3T3-E1 cells over 24 and 48 h. Cell viabilites in all groups were maintained at greater than 90% for 48 h compared with the control. Figure 5b shows the intracellular uptake of FITC/β-CD-ALG observed by CLSM. After 8 h of cultivation, FITC/β-CD-ALG was detected around the cell cytoplasm.

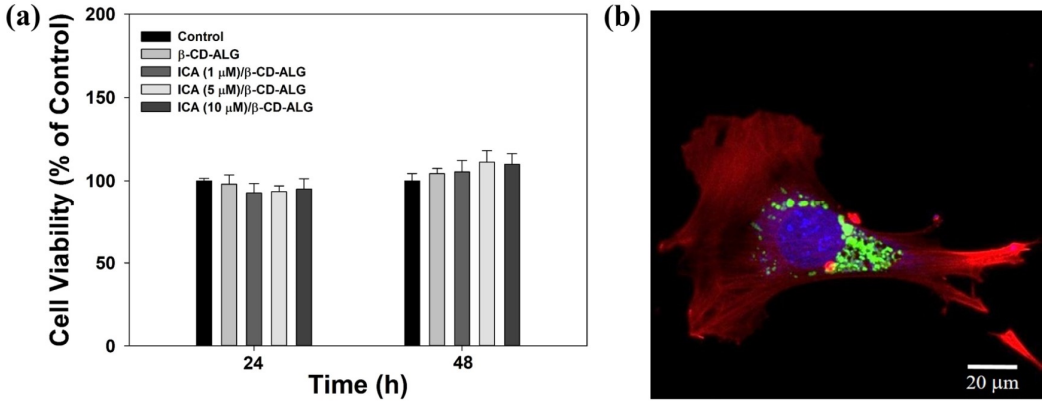

Figure 5. (**a**) Cytotoxicity test of β-CD-ALG, ICA (1 μM)/β-CD-ALG, ICA (5 μM)/β-CD-ALG, and ICA (10 μM)/β-CD-ALG on MC3T3-E1 cells. (**b**) Cellular uptake of FITC/β-CD-ALG after incubation of 8 h. Scale bar: 20 μm.

3.4. ALP Activity

To confirm the osteogenic effect of β-CD-ALG with or without ICA on MC3T3-E1 cells, we evaluated ALP activity. The ALP activities of MC3T3-E1 cells incubated with each sample remained steady during

the time-period (Figure 6). After three days, noticeable differences were not shown between the groups in the ALP levels of MC3T3-E1 cells. At nine days, the ALP level of MC3T3-E1 cells treated with ICA (10 μM)/β-CD-ALG was significantly greater than that of those treated with ICA (1 μM)/β-CD-ALG (* $p < 0.05$). In contrast, a significant difference was not observed in ALP activity between MC3T3-E1 cells cultured on ICA (5 μM)/β-CD-ALG or ICA (10 μM)/β-CD-ALG at all incubation time points.

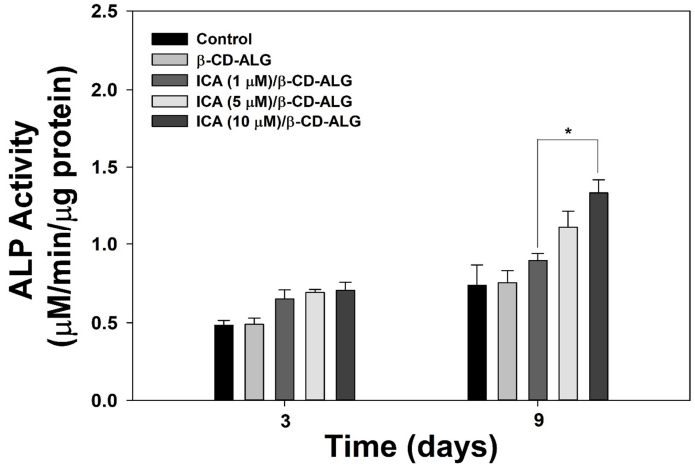

Figure 6. Analyses of ALP levels of MC3T3-E1 cells incubated with β-CD-ALG, ICA (1 μM)/β-CD-ALG, ICA (5 μM)/β-CD-ALG, and ICA (10 μM)/β-CD-ALG after 3 and 9 days of incubation (n = 4). * $p < 0.05$.

3.5. Calcium Content

The amount of calcium deposited by MC3T3-E1 cells treated with β-CD-ALG with or without ICA was measured on days 7 and 21 (Figure 7). The amount of calcium deposited by cells treated with β-CD-ALG containing ICA increased time-dependently. The amount of calcium deposited by MC3T3-E1 cells incubated with ICA (10 μM)/β-CD-ALG was greater than that by cells incubated with ICA (1 μM)/β-CD-ALG or ICA (5 μM)/β-CD-ALG for the 7-day period. Significant differences were detected in the amount of calcium deposited by MC3T3-E1 cells treated with ICA (10 μM)/β-CD-ALG and ICA (1 μM)/β-CD-ALG and between those treated with ICA (10 μM)/β-CD-ALG and ICA (5 μM)/β-CD-ALG at 21 days (* $p < 0.05$).

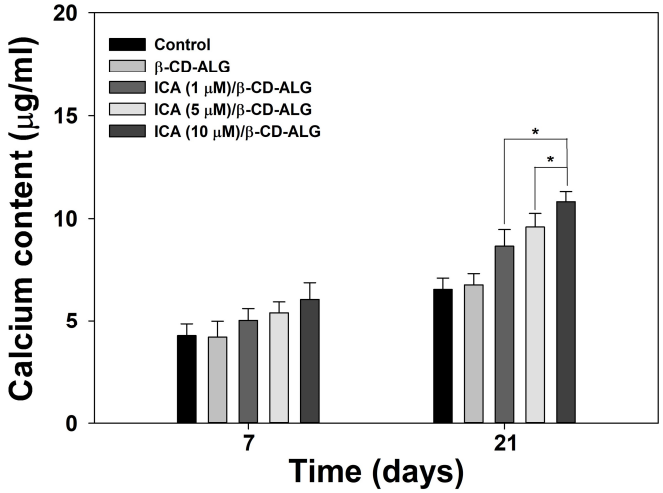

Figure 7. The deposited calcium amounts by MC3T3-E1 cells incubated with β-CD-ALG, ICA (1 μM)/β-CD-ALG, ICA (5 μM)/β-CD-ALG, and ICA (10 μM)/β-CD-ALG after 7 and 21 days of incubation (n = 4). * $p < 0.05$.

3.6. Gene Expression

To demonstrate the osteogenic differentiation effects of β-CD-ALG with or without ICA, we measured the osteogenic differentiation gene markers including OCN and OPN at 7 and 21 days. The OCN and OPN gene expression in cells treated with each sample increased slowly in a time-dependent fashion (Figure 8a,b). At day 7, the OCN and OPN gene levels in MC3T3-E1 cells on ICA (10 μM)/β-CD-ALG were substantially higher than those in cells treated with ICA (1 μM)/β-CD-ALG or ICA (5 μM)/β-CD-ALG (** $p < 0.01$ or * $p < 0.05$). Moreover, OCN and OPN mRNA levels significantly and dose-dependently increased between ICA (10 μM)/β-CD-ALG and ICA (1 μM)/β-CD-ALG treated groups at 21 days (* $p < 0.05$).

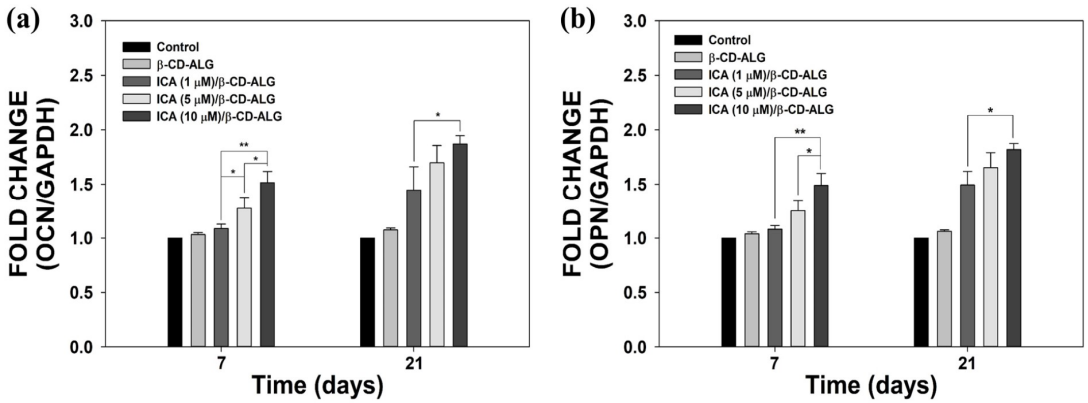

Figure 8. The gene levels of (**a**) OCN and (**b**) OPN in cells treated with β-CD-ALG, ICA (1 μM)/β-CD-ALG, ICA (5 μM)/β-CD-ALG, and ICA (10 μM)/β-CD-ALG at 7 and 21 days (n = 4). ** $p < 0.01$ and * $p < 0.05$.

4. Discussion

The present study investigated whether the osteogenic activity of MC3T3-E1 cells could be enhanced using inclusion nanocarrier of ICA and β-CD-ALG (ICA/β-CD-ALG). The particle sizes of β-CD-ALG with or without ICA measured by TEM and DLS ranged from approximately 430 to 480 nm in diameter. Kim et al. [23] demonstrated that simvastatin (SIM)-incorporated hyaluronic acid (HA)-conjugated β-CD (HA-β-CD) led to sustained release of SIM for up to 63 days. More recently, Chen et al. [24] showed that berberine chloride (BE)-loaded sulfonate-β-CD-chitosan self-assembly nanoparticle led to steady, controlled drug release. Consistent with these studies, we found that ICA release profiles from β-CD-ALG exhibited a controlled release pattern for 7 days.

Previous studies reported that ICA treatments not only promoted Runx-2 (runt-related transcription factor 2) gene levels in pre-osteoblastic MC3T3-E1 cells, but also induced expression of the Id-1 (inhibitor of DNA-binding 1) gene in mouse primary osteoblasts [25]. Previous studies demonstrated that, in combination with various materials such as porous poly(3-hydroxybutyrate-co-3-hydroxyvalerate) scaffolds, calcium phosphate cement tablets, and porous β-tricalcium phosphate ceramic disks, ICA significantly improved cell proliferation in vitro and induced new bone formation and blood vessels in vivo [26–28].

Based on the previous studies, we evaluated the osteogenic effects of ICA/β-CD-ALG on MC3T3-E1 cells via ALP activity, calcium content, and gene expression. ALP, a cell membrane-related enzyme, previously showed early expression consistent with osteoblast differentiation. Alkaline phosphatase has been widely proposed as an early osteoblast differentiation marker [29–31]. Furthermore, ALP activity has been shown to be associated with matrix development in osteoblasts before mineralization [31]. The ALP levels of MC3T3-E1 cells treated with β-CD-ALG, ICA (1 μM)/β-CD-ALG, ICA (5 μM)/β-CD-ALG, and ICA (10 μM)/β-CD-ALG were measured after days 3 and 9 of incubation. The ALP activity of MC3T3-E1 cells incubated with β-CD-ALG (regardless of ICA) increased in a time- and dose-dependent manner. After three days, ALP activity was not significantly different in

MC3T3-E1 cells treated with bare β-CD-ALG or β-CD-ALG with ICA. However, a noticeable difference was observed in ALP levels between the MC3T3-E1 cells handled with ICA (10 μM)/β-CD-ALG and those handled with ICA (1 μM)/β-CD-ALG after nine days of incubation. Calcium deposition has generally been used as a late osteogenic differentiation marker [32,33]. Thus, the amount of calcium deposited by MC3T3-E1 cells treated with β-CD-ALG with or without ICA was investigated after 7 or 21 days of cultivation. Calcium deposition of MC3T3-E1 cells cultivated with β-CD-ALG with ICA was higher than that in MC3T3-E1 cells cultivated with β-CD-ALG at 7 days. The deposited calcium contents were significantly different between MC3T3-E1 cells treated with ICA (10 μM)/β-CD-ALG and ICA (1 μM)/β-CD-ALG at 21 days. Cao et al. [34] described increased ALP activity and mineralization of MC3T3-E1 cells stimulated by ICA through up-regulation of bone morphogenetic protein-2. More recently, Huang et al. [35] showed that ICA promoted ALP activity and mineral content in MC3T3-E1 cells through microRNA-153 that targets the Runx2 pathway. These prior results were consistent with our results and imply that ICA promotes ALP activity and calcium deposition.

To further investigate osteogenic differentiation, we measured the mRNA expression levels of osteogenic differentiation markers such as OCN and OPN in MC3T3-E1 cells treated with β-CD-ALG in the presence or absence of ICA. The organic matrix of bone contains proteins such as OCN and OPN, which are important in coordinating the organic matrix and bone mineral [36]. Both OCN and OPN are well-known to upregulate osteoblast differentiation [33,37]. OCN, or bone gamma-carboxyglutamic acid-containing protein (BGLAP), is found in both bone and dentin. OPN, or bone sialoprotein I (BSP-I), is an extracellular matrix (ECM) protein. There were significant differences in OCN and OPN gene levels between MC3T3-E1 cells treated with ICA (10 μM)/β-CD-ALG and those treated with ICA (1 μM)/β-CD-ALG. The mRNA levels of OCN and OPN in cells treated with ICA (10 μM)/β-CD-ALG were higher than those of cells treated with ICA (5 μM)/β-CD-ALG. The mRNA expression level of OPN in MC3T3-E1 cells treated with 1 μM ICA for 14 days was markedly higher than that of control cells [35]. Chen et al. [38] reported that, after ICA (10 μM) treatment, the mRNA level of OCN in multipotent mesenchymal progenitor C2C12 cells was markedly up-regulated compared to the expression level in control cells. These results suggest that ICA provides both early and late osteoblast differentiation.

ICA has been applied for bone tissue engineering in vitro and in vivo. However, its application for bone regeneration is still limited due to its toxicity, poor biocompatibility, and induction of apoptosis in several cells [20]. In the current study, the delivery of ICA using a β-CD-ALG nanocarrier achieved greater osteogenic activity of MC3T3-E1 cells via sustained ICA release from nanocarrier. However, the sustained drug delivery generally showed similar or less effectiveness than the drug alone due to the relatively lower concentration of the drug by the sustained release from the delivery system. Therefore, we are carrying out bone tissue regeneration effects of ICA/β-CD-ALG on bone defect models and comparing in vivo osteogenic activity between ICA/β-CD-ALG and ICA alone.

5. Conclusions

In this study, ICA/β-CD-ALG inclusion nanocomplex was prepared via the chemical reaction of carboxylated CD with aminated ALG and ICA inclusion in the internal cavity of β-CD residues of β-CD-ALG. The ICA/β-CD-ALG inclusion nanocomplex exhibited sustained release of ICA. The ICA/β-CD-ALG inclusion nanocomplex enhanced the osteogenic potency of MC3T3-E1 cells by increasing ALP levels, the deposited calcium contents, and the expression levels of OCN and OPN via the sustained release of ICA from inclusion nanocomplex. Consequently, the ICA/β-CD-ALG inclusion nanocomplex offers great potential in regeneration and repair of bony defects and diseases.

Supplementary Materials: The following are available online at http://www.mdpi.com/2076-3417/10/12/4137/s1, Table S1: RT-PCR primer sequences of the genes related to osteogenic markers. PCR amplification and detection.

Author Contributions: Conceptualization, M.H.S., K.P., and S.E.K.; methodology, S.C. and H.-S.J.; validation, Y.S.L. and W.K.J.; formal analysis, H.-J.K., K.P., and S.E.K.; writing—original draft preparation, S.C., Y.S.L.,

and S.E.K.; writing—review and editing, H.-J.K., K.P., and S.E.K.; funding acquisition, M.H.S. All authors have read and agreed to the published version of the manuscript.

Funding: This study was supported by the Bio & Medical Technology Development Program of the National Research Foundation of Korea (NRF) funded by the Korean government, MSIP (NRF-2017M3A9B3063640) and the National Research Foundation of Korea (NRF) grant funded by the Korea government (MSIT) (No. 2018R1D1A1B07050155).

Conflicts of Interest: The authors declare no conflict of interest.

References

1. Ashammakhi, N.; Ahadian, S.; Darabi, M.A.; El Tahchi, M.; Lee, J.; Suthiwanich, K.; Sheikhi, A.; Dokmeci, M.R.; Oklu, R.; Khademhosseini, A. Minimally Invasive and Regenerative Therapeutics. *Adv. Mater.* **2019**, *31*, e1804041. [CrossRef] [PubMed]
2. Jia, Y.C.; Zhang, P.L.; Sun, Y.C.; Kang, Q.L.; Xu, J.; Zhang, C.F.; Chai, Y.M. Regeneration of large bone defects using mesoporous silica coated magnetic nanoparticles during distraction osteogenesis. *Nanomedicine* **2019**, *21*. [CrossRef] [PubMed]
3. Zimmermann, C.E.; Borner, B.I.; Hasse, A.; Sieg, P. Donor site morbidity after microvascular fibula transfer. *Clin. Oral. Investig.* **2001**, *5*, 214–219. [CrossRef] [PubMed]
4. Silber, J.S.; Anderson, D.G.; Daffner, S.D.; Brislin, B.T.; Leland, J.M.; Hilibrand, A.S.; Vaccaro, A.R.; Albert, T.J. Donor site morbidity after anterior iliac crest bone harvest for single-level anterior cervical discectomy and fusion. *Spine* **2003**, *28*, 134–139. [CrossRef] [PubMed]
5. Lewandrowski, K.U.; Rebmann, V.; Passler, M.; Schollmeier, G.; Ekkernkamp, A.; Grosse-Wilde, H.; Tomford, W.W. Immune response to perforated and partially demineralized bone allografts. *J. Orthop. Sci.* **2001**, *6*, 545–555. [CrossRef] [PubMed]
6. Jaitak, V.; Kaul, V.K.; Kumar, N.; Singh, B.; Savergave, L.S.; Jogdand, V.V.; Nene, S. Simple and efficient enzymatic transglycosylation of stevioside by beta-cyclodextrin glucanotransferase from Bacillus firmus. *Biotechnol. Lett.* **2009**, *31*, 1415–1420. [CrossRef]
7. Kurkov, S.V.; Loftsson, T. Cyclodextrins. *Int. J. Pharm.* **2013**, *453*, 167–180. [CrossRef] [PubMed]
8. Jansook, P.; Ogawa, N.; Loftsson, T. Cyclodextrins: Structure, physicochemical properties and pharmaceutical applications. *Int. J. Pharm.* **2018**, *535*, 272–284. [CrossRef]
9. Loftsson, T.; Duchene, D. Cyclodextrins and their pharmaceutical applications. *Int. J. Pharmaceut.* **2007**, *329*, 1–11. [CrossRef]
10. Devasari, N.; Dora, C.P.; Singh, C.; Paidi, S.R.; Kumar, V.; Sobhia, M.E.; Suresh, S. Inclusion complex of erlotinib with sulfobutyl ether-beta-cyclodextrin: Preparation, characterization, in silico, in vitro and in vivo evaluation. *Carbohydr. Polym.* **2015**, *134*, 547–556. [CrossRef]
11. Bragagni, M.; Bozdag, M.; Carta, F.; Scozzafava, A.; Lanzi, C.; Masini, E.; Mura, P.; Supuran, C.T. Cyclodextrin complexation highly enhances efficacy of arylsulfonylureido benzenesulfonamide carbonic anhydrase inhibitors as a topical antiglaucoma agents. *Bioorgan. Med. Chem.* **2015**, *23*, 6223–6227. [CrossRef] [PubMed]
12. Rekharsky, M.V.; Inoue, Y. Complexation Thermodynamics of Cyclodextrins. *Chem. Rev.* **1998**, *98*, 1875–1918. [CrossRef] [PubMed]
13. Irie, T.; Uekama, K. Cyclodextrins in peptide and protein delivery. *Adv. Drug Deliv. Rev.* **1999**, *36*, 101–123. [CrossRef]
14. Lysik, M.A.; Wu-Pong, S. Innovations in oligonucleotide drug delivery. *J. Pharm. Sci.* **2003**, *92*, 1559–1573. [CrossRef]
15. Khan, J.; Alexander, A.; Saraf, S.; Saraf, S. Recent advances and future prospects of phyto-phospholipid complexation technique for improving pharmacokinetic profile of plant actives. *J. Control Release* **2013**, *168*, 50–60. [CrossRef]
16. Ye, Y.; Jing, X.; Li, N.; Wu, Y.; Li, B.; Xu, T. Icariin promotes proliferation and osteogenic differentiation of rat adipose-derived stem cells by activating the RhoA-TAZ signaling pathway. *Biomed. Pharmacother.* **2017**, *88*, 384–394. [CrossRef] [PubMed]
17. Liu, H.; Li, W.; Luo, B.; Chen, X.; Wen, W.; Zhou, C. Icariin immobilized electrospinning poly(l-lactide) fibrous membranes via polydopamine adhesive coating with enhanced cytocompatibility and osteogenic activity. *Mater. Sci. Eng. C Mater. Biol. Appl.* **2017**, *79*, 399–409. [CrossRef]

18. Qin, S.; Zhou, W.; Liu, S.; Chen, P.; Wu, H. Icariin stimulates the proliferation of rat bone mesenchymal stem cells via ERK and p38 MAPK signaling. *Int. J. Clin. Exp. Med.* **2015**, *8*, 7125–7133.
19. Zhai, Y.K.; Guo, X.Y.; Ge, B.F.; Zhen, P.; Ma, X.N.; Zhou, J.; Ma, H.P.; Xian, C.J.; Chen, K.M. Icariin stimulates the osteogenic differentiation of rat bone marrow stromal cells via activating the PI3K-AKT-eNOS-NO-cGMP-PKG. *Bone* **2014**, *66*, 189–198. [CrossRef]
20. Li, M.; Zhang, C.; Zhong, Y.; Zhao, J.Y. A Novel Approach to Utilize Icariin as Icariin-Derived ECM on Small Intestinal Submucosa Scaffold for Bone Repair. *Ann. Biomed. Eng.* **2017**, *45*, 2673–2682. [CrossRef]
21. Lee, K.Y.; Mooney, D.J. Alginate: Properties and biomedical applications. *Prog. Polym. Sci.* **2012**, *37*, 106–126. [CrossRef]
22. Pawar, S.N.; Edgar, K.J. Alginate derivatization: A review of chemistry, properties and applications. *Biomaterials* **2012**, *33*, 3279–3305. [CrossRef] [PubMed]
23. Kim, T.H.; Yun, Y.P.; Shim, K.S.; Kim, H.J.; Kim, S.E.; Park, K.; Song, H.R. *In Vitro* Anti-Inflammation and Chondrogenic Differentiation Effects of Inclusion Nanocomplexes of Hyaluronic Acid-Beta Cyclodextrin and Simvastatin. *Tissue Eng. Regen. Med.* **2018**, *15*, 263–274. [CrossRef] [PubMed]
24. Chen, X.M.; Chen, Y.; Hou, X.F.; Wu, X.; Gu, B.H.; Liu, Y. Sulfonato-beta-Cyclodextrin Mediated Supramolecular Nanoparticle for Controlled Release of Berberine. *ACS Appl. Mater. Interfaces* **2018**, *10*, 24987–24992. [CrossRef] [PubMed]
25. Zhao, J.; Ohba, S.; Shinkai, M.; Chung, U.I.; Nagamune, T. Icariin induces osteogenic differentiation in vitro in a BMP- and Runx2-dependent manner. *Biochem. Biophys. Res. Commun.* **2008**, *369*, 444–448. [CrossRef]
26. Xia, L.; Li, Y.; Zhou, Z.; Dai, Y.; Liu, H.; Liu, H. Icariin delivery porous PHBV scaffolds for promoting osteoblast expansion in vitro. *Mater. Sci. Eng. C Mater. Biol. Appl.* **2013**, *33*, 3545–3552. [CrossRef] [PubMed]
27. Zhang, X.; Guo, Y.; Li, D.X.; Wang, R.; Fan, H.S.; Xiao, Y.M.; Zhang, L.; Zhang, X.D. The effect of loading icariin on biocompatibility and bioactivity of porous beta-TCP ceramic. *J. Mater. Sci. Mater. Med.* **2011**, *22*, 371–379. [CrossRef] [PubMed]
28. Zhao, J.; Ohba, S.; Komiyama, Y.; Shinkai, M.; Chung, U.I.; Nagamune, T. Icariin: A potential osteoinductive compound for bone tissue engineering. *Tissue Eng. Part A* **2010**, *16*, 233–243. [CrossRef]
29. Zhu, L.; Ye, X.; Tang, G.; Zhao, N.; Gong, Y.; Zhao, Y.; Zhao, J.; Zhang, X. Biomimetic coating of compound titania and hydroxyapatite on titanium. *J. Biomed. Mater. Res. A* **2007**, *83*, 1165–1175. [CrossRef] [PubMed]
30. Serigano, K.; Sakai, D.; Hiyama, A.; Tamura, F.; Tanaka, M.; Mochida, J. Effect of cell number on mesenchymal stem cell transplantation in a canine disc degeneration model. *J. Orthop. Res.* **2010**, *28*, 1267–1275. [CrossRef] [PubMed]
31. Luu, H.H.; Song, W.X.; Luo, X.; Manning, D.; Luo, J.; Deng, Z.L.; Sharff, K.A.; Montag, A.G.; Haydon, R.C.; He, T.C. Distinct roles of bone morphogenetic proteins in osteogenic differentiation of mesenchymal stem cells. *J. Orthop. Res.* **2007**, *25*, 665–677. [CrossRef] [PubMed]
32. Lee, D.W.; Yun, Y.P.; Park, K.; Kim, S.E. Gentamicin and bone morphogenic protein-2 (BMP-2)-delivering heparinized-titanium implant with enhanced antibacterial activity and osteointegration. *Bone* **2012**, *50*, 974–982. [CrossRef] [PubMed]
33. Kim, S.E.; Yun, Y.P.; Shim, K.S.; Park, K.; Choi, S.W.; Shin, D.H.; Suh, D.H. Fabrication of a BMP-2-immobilized porous microsphere modified by heparin for bone tissue engineering. *Colloids Surf. B Biointerfaces* **2015**, *134*, 453–460. [CrossRef] [PubMed]
34. Cao, H.; Ke, Y.; Zhang, Y.; Zhang, C.J.; Qian, W.; Zhang, G.L. Icariin stimulates MC3T3-E1 cell proliferation and differentiation through up-regulation of bone morphogenetic protein-2. *Int. J. Mol. Med.* **2012**, *29*, 435–439. [CrossRef]
35. Huang, Z.F.; Cheng, C.; Wang, J.; Liu, X.Z.; Wei, H.; Han, Y.; Yang, S.H.; Wang, X. Icariin regulates the osteoblast differentiation and cell proliferation of MC3T3-E1 cells through microRNA-153 by targeting Runt-related transcription factor 2. *Exp. Ther. Med.* **2018**, *15*, 5159–5166. [CrossRef] [PubMed]
36. Blair, H.C.; Larrouture, Q.C.; Li, Y.; Lin, H.; Beer-Stoltz, D.; Liu, L.; Tuan, R.S.; Robinson, L.J.; Schlesinger, P.H.; Nelson, D.J. Osteoblast Differentiation and Bone Matrix Formation *In Vivo* and *In Vitro*. *Tissue Eng. Part B Rev.* **2017**, *23*, 268–280. [CrossRef]
37. Kim, S.E.; Yun, Y.P.; Lee, J.Y.; Shim, J.S.; Park, K.; Huh, J.B. Co-delivery of platelet-derived growth factor (PDGF-BB) and bone morphogenic protein (BMP-2) coated onto heparinized titanium for improving osteoblast function and osteointegration. *J. Tissue Eng. Regen. Med.* **2015**, *9*, E219–E228. [CrossRef]

38. Chen, M.; Cui, Y.; Li, H.; Luan, J.; Zhou, X.; Han, J. Icariin Promotes the Osteogenic Action of BMP2 by Activating the cAMP Signaling Pathway. *Molecules* **2019**, *24*, 3875. [CrossRef]